

Synthesis And Characterization Of Various Polymer Assisted Silver Nano Particles

N. Punitha^{a*}, R. Mohan^b, C. Rakkappan^c, and V. Venkatasubbian^d

^{a*}Department of Physics, St. Joseph's College of Engineering, Chennai – 600 119, India.

^bDepartment of Physics, School of Engineering and Technology, Surya Group of Institutions, Vikiravandi

^cDepartment of Physics, Annamalai University 608 002, Tamil Nadu, India.

^dDepartment of Physics, S.B.K. College, Aruppukottai – 626101.

Abstract: Silver nano particles were simply synthesized by chemical reduction method. Silver Nitrate ($AgNO_3$) is used as a base material and polyethylene glycol (PEG), polyethylene oxide (PEO) and polymethyl methacrylate (PMMA) were used as stabilizers along with sodium citrate as reducing agent. The well organized silver nano particles in polymers were obtained at certain concentration ratio of polymers to silver nitrate at temperature below its decomposition ($300^\circ C$). At all other concentrations the silver particles were polydispersed due to imperfect confinement. The SEM pictures reveal that the different stabilizers give rise to different shapes which vary from spherical to wire like to flaky ones. The biodegradable chitosan polymer seems to have more size control capacity than the other synthetic polymers.

Keywords: Silver nano particles, SEM, stabilizers

I. Introduction

Noble metal nano particles have been prepared in last two decades, especially for biomedical, analytical and bio analytical purposes [1-4]. Among these nano materials silver nano particles have received much attention due to their attractive physicochemical properties especially its anti bacterial activity. The antibacterial activity of silver species has been well known since ancient times [5] and it has been demonstrated that, in low concentrations, silver is non toxic to human cells [6]. It is established that Ag ions and Ag-based compounds are highly toxic to microorganisms, showing strong biocidal effects on as many as 12 species of bacteria [7]. For this reason silver-based compounds have been used extensively in many bactericidal applications [8]. The inorganic composites with a slow silver release rate that are currently used in drug delivery and preservatives in a variety of products. The antimicrobial efficiency of SNPs results from their high surface area to volume ratio. With a decrease in particle size, the amount of silver atoms exposed to the surrounding medium significantly increases, which enhances the release of silver ions with reduced reaction time. Reducing the particle size of materials is an efficient and reliable tool for improving silver nanoparticle biocompatibility. In fact, nanotechnology helps in overcoming the limitations of size and can change the outlook of the world regarding science [9]. Furthermore, nanomaterials can be modified for better efficiency to facilitate their applications in different fields such as medicine and bioscience.

The noble metal nanoparticles were mainly produced by reduction and stabilized by various methods [10-11] in which classical colloid methods [12-13] are combined with modern nanotechnology leading to many procedures for particle preparation, control of particle size, and surface modification [14-16]. The surfactants and polymers are used to prevent the metal particles nucleation and further growth through steric hindrance. In the present investigation, SNPs are synthesized by green chemical route [17] which is simple and convenient method for preparing metal particles in the required sizes.

Nanoparticle synthesis and the study of their size and properties is of fundamental importance for further applications and its characteristics improvement such as electronic, optical, magnetic, and catalytic properties [18]. The selection of an appropriate reducing agent and nontoxic stabilizer for the stability of SNPs in the green chemical route synthesis is a crucial problem because size, shape and size distribution strongly depend on the nature of reducing and stabilizing agents [19]. Metal nanoparticles prepared by the mild reducing agents are relatively more stable compared with those produced by excess of strong reducing agents [20]. The aim was to control the growth of SNPs with the help of biodegradable polymers which are non toxic, environmental friendly and biocompatible.

The polymers chosen for the synthesis of SNPs are the three synthetic polymers viz., PEO, PEG and PMMA. Out of these four polymers, PEG and PMMA are relatively milder reductants of silver ions, which can also act as stabilizers. Hence these polymer assisted SNPs are synthesized and their characteristic features are thoroughly analyzed for choosing suitable passivating agent for preparation of nano bio composite.

II. Experimental Section

2.1 Materials

Silver Nitrate (AgNO_3) was purchased from Sigma-Aldrich. Sodium citrate, all the polymers viz., PEG, PEO and PMMA, ethanol and deionized water were purchased from Sd-fine and used without any further purification since they were analytical reagent grade with 99% purity.

2.2 Synthesis of silver nanoparticles

Synthesis of various polymers assisted SNPs were achieved by a simple and widely used chemical reduction technique [21]. 0.1 M of silver nitrate solution was prepared in deionized water and to which 0.1M sodium citrate solution was added drop by drop to change colorless solution in to pale white colour. The polymer solution prepared at 2 different concentrations (0.5 and 2 wt %) was mixed with this AgNO_3 and sodium citrate solution and stirred continuously for 24 h using a magnetic stirrer until silver ions were reduced to silver metal in nano dimensional range. Then the solution was kept at 300°C for 10 min till the samples turned into yellowish brown colour which indicates the formation of silver nano particles. The precipitate was collected, filtered and washed several times using deionized water and ethanol. Then the precipitate was annealed at 60°C for 4 h.

III. Characterization Techniques

Absorption spectra were recorded on UV-Visible spectrophotometer (SHIMADZU-UV 1800), employing the deionized water as the reference. The crystallinity, crystal phase and particle size of the synthesized product were examined by X'pert PRO X-ray diffractometer measured with CuK radiations. Functional group confirmations were assessed by NICOLET iS5 spectrophotometer in the range $4000\text{-}400\text{ cm}^{-1}$. The photoluminescence (PL) emission spectra were recorded using VARIAN-DFC2500 spectrophotometer in the wavelength range from 330 to 550 nm at room temperature. The particle size and shape were confirmed using JEOL HR-TEM.

IV. Results And Discussion

4.1 Optical Analysis (UV-Visible)

The UV-Vis absorption spectra of nano particle colloids play an important role in assessing the shape, size and size distribution of the nanoparticles. The MNPs Surface Plasmon Resonance (SPR) peak intensity, shifting and full width half maximum data are very sensitive to the particle size and environment [22]. In this study, the UV-Vis absorption spectra of pure SNP and different polymer stabilized SNPs at low and high concentrations of polymers are presented in Figs. 4.1 to 4.3. From the careful analysis of the spectra, all samples present a single characteristics SPR band of SNPs in addition to polymer absorption peaks at lower and higher wavelength. It was observed that absorption spectrum of uncapped and polymer capped SNP samples present a maximum between 390 nm-410 nm. The polymer stabilized samples showed a marked blue shift with respect to uncapped SNP. The blue shift was found to be quite remarkable in the PEG stabilized samples when compared to other synthetic polymer stabilized samples. In the synthetic polymer stabilized samples the PMMA capped SNPs show better peak quality, intensity and blue shift of SPR band. By increasing the concentration of the polymers the intensity of the absorption peak of SNPs was found increase in all the system.

From the above observations and the colour change of pale white solution into pale brown on the formation of SNPs was attributed to the plasmon resonance induced by the interaction between the incident light and conduction electrons of SNPs. Single absorption band appeared in the range of 390-410 nm in the samples confirms the spherical nature of small sized SNPs ($< 20\text{nm}$) in the polymer stabilized solutions [23]. According to Mie's theory only a single SPR band is expected in the absorption spectra of spherical metal nanoparticles, whereas anisotropic particles could give rise to two or more SPR bands depending on the shape of the particles.

With the increased polymer concentration the SPR band enhanced gradually and also blue shifted indicate that particle size diminished when polymer concentration was increased. According to the theory proposed by **de Gennes (1976)** the conformation of polymer in a solution changes according to its critical concentration (c^*), above which polymer chains interpenetrate to form a network and below which these chains separate to behave as single coils. For high molecular weight polymer, the c^* is very small because the c^* depends on the chain length. Based on this theory the entangled conformation of polymers excludes the possibility of formation of agglomerates during the phase transfer.

The increase in the intensity of SPR band for the phase transferred nanostructure was due to its higher concentration of particles [24]. Hence it was evident that 2 wt % concentrations of PEG and PMMA have the effective phase transferred nanostructure than the other polymer concentration samples. In addition the amide group of hydroxyl terminal of PEG and acrylate terminal of PMMA also played the vital role in the reduction of silver ions. **Liz-Marzan** have proposed the reduction of silver ions by PEG occur through the oxidation of

hydroxyl terminal groups to aldehyde groups. In the case of PMMA, the reduction ability of the functional groups NH₂ and OH in silver systems were reported by Dongwei [25].

4.2 Structural Analysis (XRD)

The structure of prepared SNPs has been investigated by X-ray diffraction analysis. Typical XRD patterns of the samples are presented in Fig. 4.4 to 4.6. The diffractogram shows peaks corresponding to elemental silver in addition to some weak peaks at lower angles corresponding to the amorphous polymer base. By the observation of X-ray pattern it is clear that, both uncapped and polymer capped SNPs are having peaks appearing at 2 values 37.6°, 44.3°, 64.2° and 77.1° corresponding to (111), (200), (220) and (311) planes respectively which matches the FCC structure of bulk silver (JCPDS 04-0783). The peak at 2 values 37.6°, 44.3° associated with the crystal phases of (111) and (200) of Ag become more obvious, broadened and intense upon increasing the concentration of polymer indicate the formation of SNPs in the polymer matrices along the particular directions. These results are in agreement with the standard values and confirm the Ag reduction and growth [26]. The mean size of SNPs was estimated by analyzing the broadening of (111) reflection. The mean particle size was calculated by Debye Scherrer equation and are presented in Table 4.1.

$$D = \frac{k\lambda}{\beta \cos\theta} \quad \text{----- (1)}$$

Where λ is wave length of X-Ray (0.1541 nm), β is FWHM (full width at half maximum), θ is the diffraction angle and D is particle diameter size. It is obvious from the Table 4.1 that the polymer PEG assisted SNPs have the lower particle size (12 nm) when compared to other synthetic polymers. Out of the three synthetic polymer samples PMMA have shown better reduction of size (18 nm) than the other two polymers. The reason may be that both PEG and PMMA have the better ability of reduction and stabilization than the other two polymers. The Table 4.1 shows the value, the full width half maximum (FWHM) value and its related lattice parameters for different polymer assisted SNPs. It was evident that, as the polymer concentration was increased the lattice constant and interplanar distance decreased which would lead to the increased diffraction angle compared with pure SNP. The decrease in lattice parameter results in smaller atomic radius and hence the particle size. This is in consistent with other experimental results of polymer capped metal nanoparticles. Of all the three polymers, the polymer (PEG) seems to inhibit the particle agglomeration than any other synthetic polymers, which is obvious from the calculated values such as d , and Sa/V .

4.3 Spectral Analysis (FT-IR)

FT-IR measurement were carried out to identify the possible polymer functional groups responsible for the reduction of silver ions and capping of the reduced SNPs. Figs.4.7 to 4.9 shows the IR spectra of pure silver and polymer assisted SNPs at low and high concentrations. A very strong absorption peak was observed at 1590 cm⁻¹ in all the spectra, which was mainly due to the silver gluconate in the samples [27]. This peak was found to be very intense in the case of PEG, PEO and PMMA samples. In all the samples the C-H deformation vibration peaks at 1390 cm⁻¹ and 1328 cm⁻¹ were observed. As the concentration of the polymer was increased these peak intensities gradually get enhanced. The shift was observed from 3450 cm⁻¹ in the Ag loaded polymer spectra. This shift indicates the binding of SNPs to N-H and OH bonds of polymers [28]. This shift was well pronounced in the PEG, PEO and PMMA samples. Such an observation was made for PEG mediated SNPs [29]. In addition, the presence of less intense peaks at lower wave numbers at 540 cm⁻¹ and 405 cm⁻¹ related to the SNPs bonding with oxygen from OH groups of polymer molecules. From the interpretations of the FT-IR spectra it was evident that polymer molecules were present on the surface of the SNPs which prevent the agglomeration of silver ions and lead to smaller size NPs in the polymer assisted nanostructures.

4.4 Microscopic Analysis (HR-TEM)

It has been extensively reviewed and proposed that HR-TEM is one of the most efficient and versatile tools for the characterization of nanoscale materials and essential in size and shape analysis of the prepared particles [30]. The representative HR-TEM monographs are given in Fig. 4.10 (a-b) for PEG and PMMA capped SNPs respectively. It can be seen that PEG assisted SNPs are approximately spherical and reasonably monodispersed with average diameter in the range from 8-10 nm. However the PEG assisted SNPs displayed a somewhat pseudospherical faceted shape with average particle diameter around 10-12 nm. Both the particle sizes determined by HR-TEM were found to be in agreement with the pervious characterization studies.

4.5 Photoluminescence Study (PL)

The Photoluminescence emission spectra of PEG capped and PMMA capped SNPs are shown in Fig. 4.11 and 4.12. From the spectra it can be noticed that the polymer capped SNPs have emission peaks at 495 and 545 nm as in pure silver samples but the emission intensity is enhanced in the polymer capped samples without any shift in the peak. These emission peaks of Ag occurred due to radiative recombination of electron hole pairs between d-band and sp-conduction above Fermi level [31]. The enhancement of these peaks in the PEG and PMMA coated samples indicate that the silver ions are very well dispersed and more number of electron hole

recombination process occurred on its surface [32]. Hence it is concluded that 2 wt % concentrations of PEG and PMMA showed the very good optical behavior which confirmed the SNPs were highly passivated in this particular concentration and in the particular polymer.

V. Conclusion

SNPs have been synthesized using different synthetic polymers and a biodegradable polymer. The synthetic scheme which was followed is a simple and effective chemical reduction method. The SPR band noticed in the characteristic silver region confirmed the formation of the SNPs. Molecular interactions and phase morphology were characterized using FT-IR and XRD. The PL behavior was enhanced in PEG and PMMA capped SNPs due to the increased radiative recombination process on silver ion surface. The PEG and PMMA were used simultaneously as reducing and passivating agent which results in SNPs of uniform size less than 15nm was confirmed by XRD analysis. Future works using different combination of biopolymers can be embarked to further elucidate the stabilization of the nanoparticles. The successful synthesis of SNPs by these polymers lead to a fact that 2 wt % concentrations of PMMA capped SNPs can be useful in developing metal nano biocomposites which has wide application in biomedicine.

Reference

- [1] Elechiguerra, J.L., Burt, J.L., Morones, J.R., **2005**, *J. Nanobiotech.*, Vol. 3 (6) pp.1186-1195.
- [2] Sioss, J.A., Stoermer, R.L., Sha, M.Y., Keating, C. D., **2007**, *Langmuir*, Vol. 23, pp.11334-11341.
- [3] Yang, T., Li, Z., Wang, L., Guo, C., Sun, Y., **2007**, *Langmuir*, Vol. 23, pp. 10533-10538.
- [4] Huang, C.J, Shieu, F.S., **2005**, *Colloid Polym. Sci.*, Vol. 284, pp.192-202.
- [5] Shrivastava, S., Bera, T., Roy, A., Singh, G., Ramachandrarao, P., Dash, D., **2007**, *Nanotech.*, Vol.18, pp. 225103-225111.
- [6] Pal, A., Esumi, K., Pal, T., **2005**, *J.Colloid Interface Sci.*, Vol.288, pp. 396-401.
- [7] Zhao, G., Stevens, S.E., **1998**, *Biometals.*, Vol. 11, pp. 27-32.
- [8] Morones, J.R., Elechiguerra, J.L., Camacho, A., Holt, K., Kouri, J.B., Ram rez, J.T., Yacamán M.J., **2005**, *Nanotech.*, Vol. 16, pp.2346-2353.
- [9] Mirkin, C.A., Taton, T.A., **2000**, *Nature*, Vol.405, pp. 626-627.
- [10] Papp, S., Dekany, I., **2001**, *Colloid Polym. Sci.*, Vol. 279, pp.449-458.
- [11] Creighton, J.A., Blatchford, C.G., Albrecht, M.G., **1979**, *J. Chem. Soc.Faraday Trans.*, Vol.75, pp.790-798.
- [12] Lee, P.C., Miesel, D., **1982**, *J. Phys. Chem.*, Vol.86 (17), pp.3391-3395.
- [13] Bell, W.C., Myrick, M.L., **2001**, *J. Colloid Inter. Sci.*, Vol. 242, pp.300-305.
- [14] Beversluis, M.R., Bouhelier, A., Novotny, L., **2003**, *Phys. Rev. B*, Vol. **68**, pp.115433-115443.
- [15] He, F., Zhao, D., Liu, J., **2007**, *Ind. Eng. Chem. Res.*, Vol. 46, pp. 29-34.
- [16] Wang, X., Zhuang, J., Peng, Q., Li, Y., **2005**, *Nature*, Vol.437, pp.121-124.
- [17] Cao, X.L., Cheng, C., Ma Y.L., Zhao, C.S., **2010**, *Mater Sci. Mater Med.*, Vol. 21, pp. 2861-2868.
- [18] Chang, C. C., Chen, J.Y., Hsu, T. L., Lin, C.K, Chan, C.C., **2008**, *Thin Sol.Films*, Vol. 516, pp.1743-1747.
- [19] Henglein, A., **1993**, *J. Phys.Chem.*, Vol. 97(21), pp. 5457-5471.
- [20] Heinzman, S.W., Gamem, B., **1982**, *J. Am. Chem. Soc.*, Vol.104, pp. 6801-6802.
- [21] Banerjee, A.N., Chattopadhyay, K.K., Depla, D., Maheiu, S., **2008**, (Eds.), Berlin, Heidelberg.
- [22] Huang, H., Yang, X., **2004**, *Biomacromol.*, Vol. 5, pp. 2340-2346.
- [23] He, R., Qian, X., Yin, J., Zhu, Z., **2002**, *J. Mater. Chem.*, Vol.12, pp. 3783-3786.
- [24] Novak, J.P., Feldheim, D.L., **2000**, *J. Am. Chem. Soc.*, Vol. 122, pp. 3979-3980.
- [25] De, B. M., Ghosh, P. S., Rotello, V. M., **2008**, *Adv. Mater.*, Vol. 20, pp. 4225-4241.
- [26] Hu, M., Chen, J., Li, Z.Y., Au, L., Hartland, G.V., Li, X., Marquez, M., Xia, Y., **2006**, *Chem. Soc. Rev.*, Vol. 35, pp. 1084-1094.
- [27] Carmen, R., Airinei, A., Stoica, I., Ioanid, A., **2010**, *J. Nanopart. Res.*, Vol.12, pp. 2163-2177.
- [28] Philip, D., **2009**, *Spectrochim. Acta A Mol. Biomol. Spectrosc.*, Vol.73, pp.650-653.
- [29] Kumar, H., Rani, R., **2013**, *Inter. J. Engg. Innvo. Tech.*, Vol.3, pp. 344-348.
- [30] Williams, D.B., Carter, C.B., **2009**, *A Textbook for Materials Science*, Springer, pp. 3-22.
- [31] Treguer, M., Rocco, F., Lelong, G., Nestour, A.L., Cardinal, T., Maali, A., Lounis, B., **2005**, *Sol. St. Sci.*, Vol.7, pp. 812-818.
- [32] Bouheiler, A., Beversluis, M.R., Novonty, L., **2003**, *Appl. Phy. lett.* Vol.83(24), pp. 5041-5043.

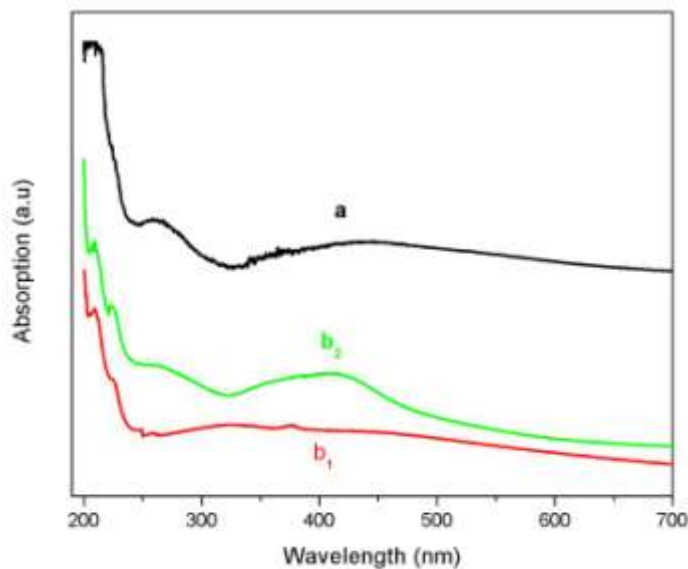


Fig. 4.1 UV-Vis absorption spectra of (a) Pure Ag and PEG capped (b₁-0.5% and b₂-2%) SNPs.

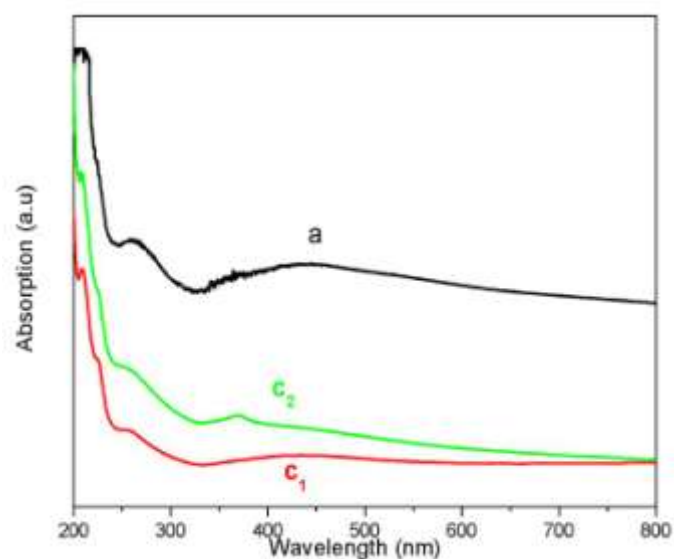


Fig. 4.2 UV-Vis absorption spectra of (a) Pure Ag and PEO capped (c₁-0.5% and c₂-2%) SNPs.

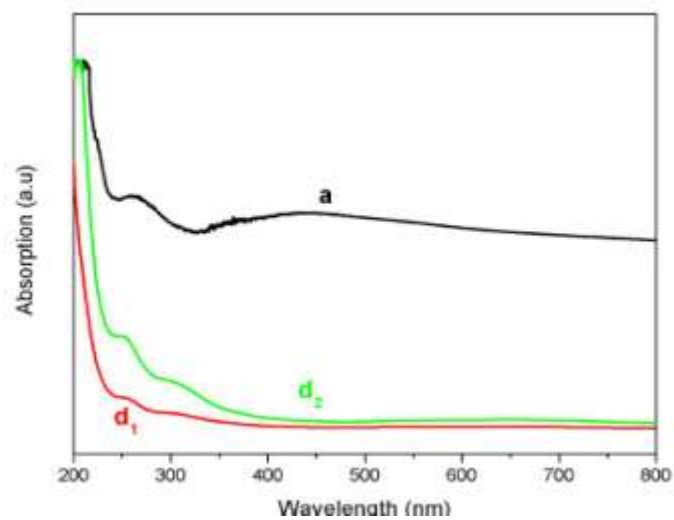


Figure 4.3 UV-Vis absorption spectra of (a) Pure Ag and PMMA capped (d₁-0.5% and d₂-2%) SNPs

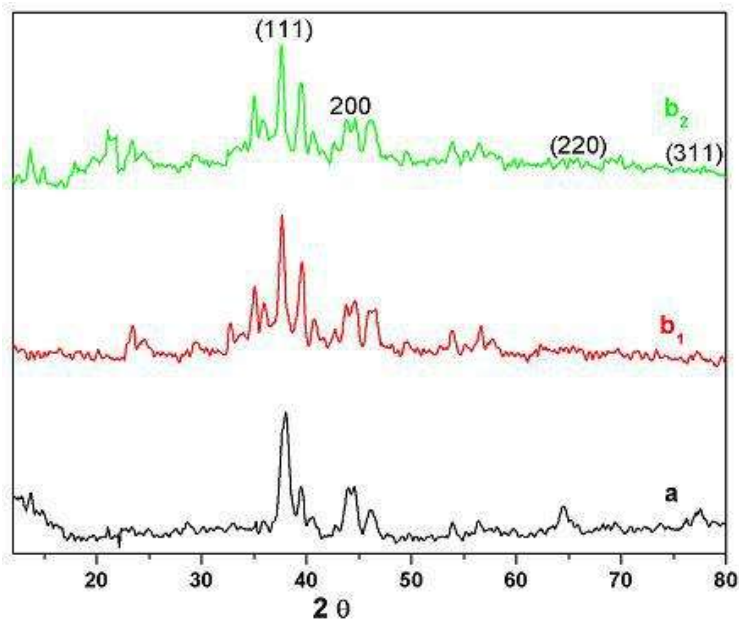


Figure 4.4 XRD spectra of (a) Pure Ag and PEG capped (b₁-0.5% and b₂-2%) SNPs

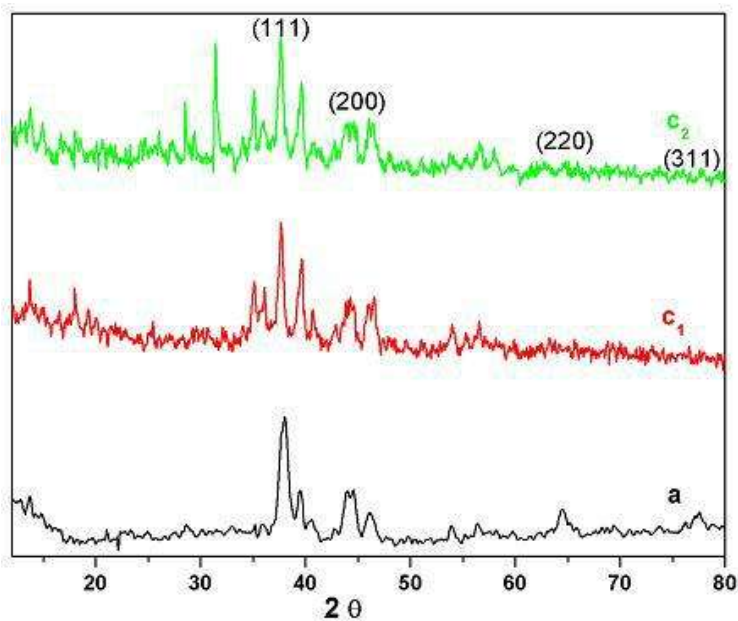


Figure 4.5 XRD spectra of (a) Pure Ag and PEO capped (c₁-0.5% and c₂-2%) SNPs.

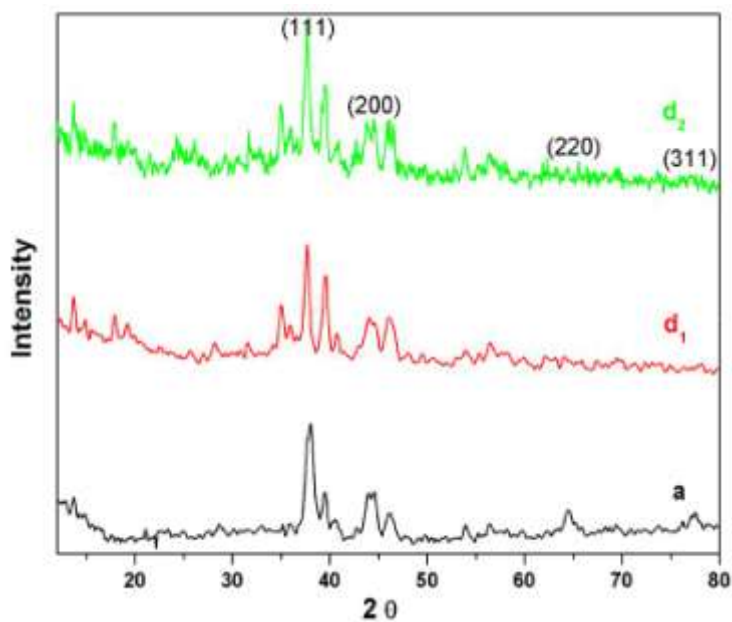


Figure 4.6 XRD spectra of (a) Pure Ag and PMMA capped (c₁-0.5% and c₂-2%) SNPs

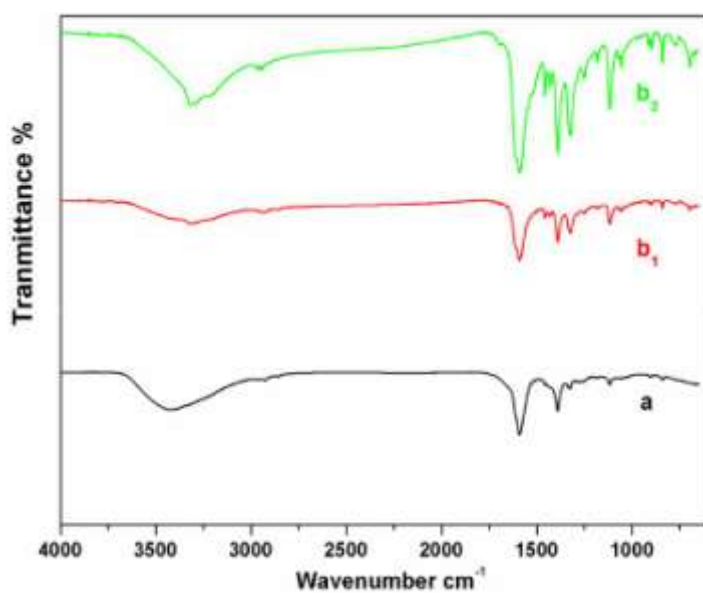


Figure 4.7 FT-IR spectra of (a) Pure Ag and PEG capped (b₁-0.5% and b₂-2%) SNPs.

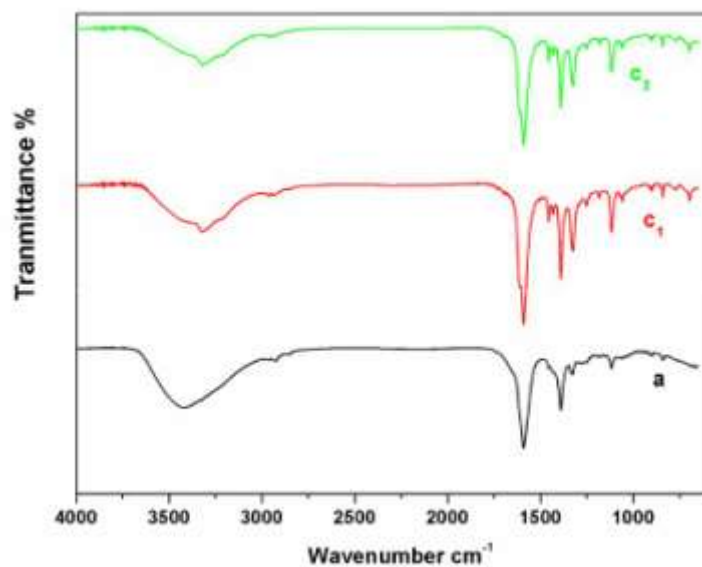


Figure 4.8 FT-IR spectra of (a) Pure Ag and PEO capped (c₁-0.5% and c₂-2%) SNPs.

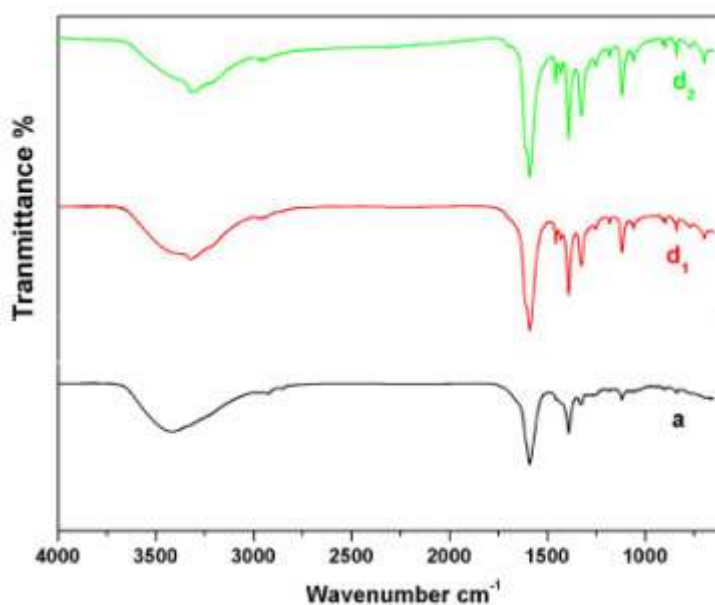


Figure 4.9 FT-IR spectra of (a) Pure Ag and PMMA capped (d₁-0.5% and d₂-2%) SNPs

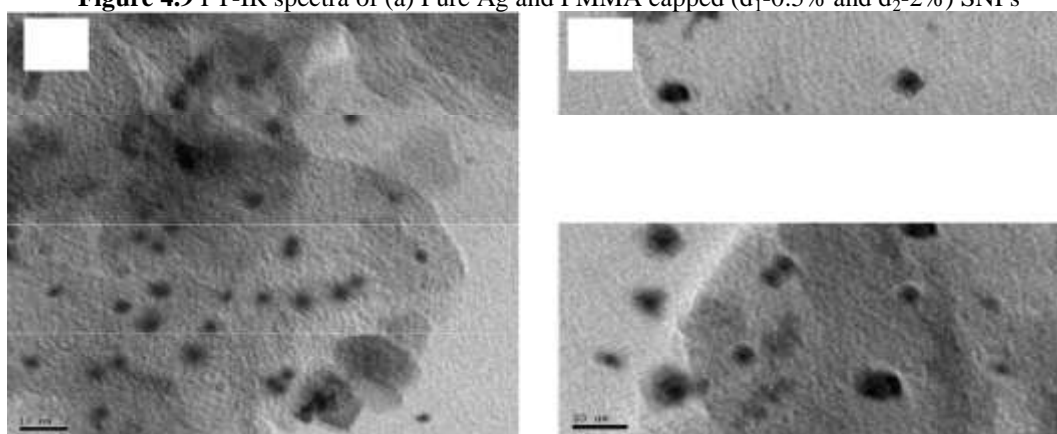


Figure 4.10 HR-TEM image of polymer capped SNPs.[a-PEG (2%) and b-PMMA (2%)].

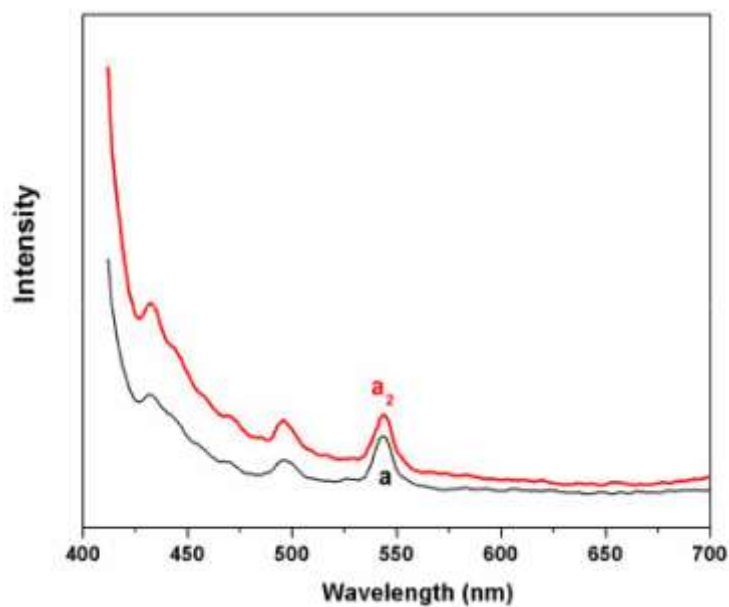


Figure 4.11 PL spectra of (a) Pure Ag and PEG capped (a₂-2%) SNPs

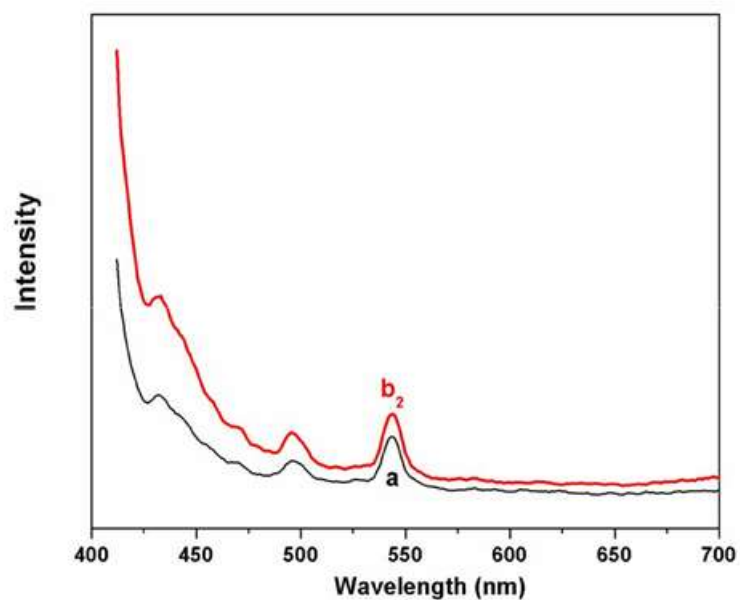


Figure 4.12 PL spectra of (a) Pure Ag and PMMA capped (b₂-2%) SNPs.